



Haworth, J., Jenkinson, H., Petersen, H., Back, C., Brittan, J., Kerrigan, S., & Nobbs, A. (2017). Concerted functions of *Streptococcus gordonii* surface proteins PadA and Hsa mediate activation of human platelets and interactions with extracellular matrix. *Cellular Microbiology*, 19(1), [e12667].
<https://doi.org/10.1111/cmi.12667>

Publisher's PDF, also known as Version of record

License (if available):
CC BY

Link to published version (if available):
[10.1111/cmi.12667](https://doi.org/10.1111/cmi.12667)

[Link to publication record in Explore Bristol Research](#)
PDF-document

This is the final published version of the article (version of record). It first appeared online via Wiley at <http://onlinelibrary.wiley.com/doi/10.1111/cmi.12667/abstract>. Please refer to any applicable terms of use of the publisher.

University of Bristol - Explore Bristol Research

General rights

This document is made available in accordance with publisher policies. Please cite only the published version using the reference above. Full terms of use are available:
<http://www.bristol.ac.uk/red/research-policy/pure/user-guides/ebr-terms/>

ORIGINAL ARTICLE

Concerted functions of *Streptococcus gordonii* surface proteins PadA and Hsa mediate activation of human platelets and interactions with extracellular matrix

Jennifer A. Haworth¹ | Howard F. Jenkinson¹ | Helen J. Petersen^{1†} | Catherine R. Back¹ | Jane L. Brittan¹ | Steve W. Kerrigan² | Angela H. Nobbs¹

¹School of Oral and Dental Sciences, University of Bristol, Bristol, UK

²Cardiovascular Infection Group, Royal College of Surgeons in Ireland, Dublin 2, Ireland

Correspondence

Dr Angela H. Nobbs, Oral Microbiology Laboratories, School of Oral and Dental Sciences, University of Bristol, Lower Maudlin Street, Bristol BS1 2LY, United Kingdom. Email: angela.nobbs@bristol.ac.uk

Summary

A range of *Streptococcus* bacteria are able to interact with blood platelets to form a thrombus (clot). *Streptococcus gordonii* is ubiquitous within the human oral cavity and amongst the common pathogens isolated from subjects with infective endocarditis. Two cell surface proteins, Hsa and Platelet adherence protein A (PadA), in *S. gordonii* mediate adherence and activation of platelets. In this study, we demonstrate that PadA binds activated platelets and that an NGR (Asparagine-Glycine-Arginine) motif within a 657 amino acid residue N-terminal fragment of PadA is responsible for this, together with two other integrin-like recognition motifs RGT and AGD. PadA also acts in concert with Hsa to mediate binding of *S. gordonii* to cellular fibronectin and vitronectin, and to promote formation of biofilms. Evidence is presented that PadA and Hsa are each reliant on the other's active presentation on the bacterial cell surface, suggesting cooperativity in functions impacting both colonization and pathogenesis.

1 | INTRODUCTION

Streptococcus, *Staphylococcus*, and *Enterococcus* bacteria account for >80% cases of infective endocarditis (Muñoz et al., 2015; Slipczuk et al., 2013) and are able to trigger activation or aggregation of blood platelets into a clot or thrombus (Fitzgerald, Foster, & Cox, 2006; Kerrigan, 2015). Viridans-group streptococci that enter the bloodstream in otherwise healthy subjects almost always originate from the complex microbial communities present within the human oral cavity (Cahill & Prendergast, 2015; McNicol & Israels, 2010; Nilson, Olaison, & Rasmussen, 2015). Accordingly, there is a predictive link between levels of oral hygiene and the risk of cardiovascular disease (Lockhart et al., 2009). Platelet adhesion and activation by oral streptococci occurs by several different mechanisms (Cognasse et al., 2015; Kerrigan & Cox, 2010; McNicol, 2015). For *Streptococcus gordonii*, *S. oralis* and *S. sanguinis*, a common primary interaction occurs with platelet integrin receptor GPIb mediated by a bacterial surface serine-rich repeat protein (Deng et al., 2014). In *S. sanguinis*,

a direct interaction between serine-rich repeat protein SrpA and GPIbA leads to platelet rolling over immobilized bacteria and adhesion at low shear (Kerrigan et al., 2002; Plummer et al., 2005). *S. gordonii* serine-rich repeat glycoprotein designated Hsa (Takahashi, Konishi, Cisar, & Yoshikawa, 2002), or GspB (Bensing & Sullam, 2002), seems to act in a similar manner (Bensing, López, & Sullam, 2004; Kerrigan et al., 2007). Hsa and GspB recognize structurally-distinct sialic acid-oligosaccharides on GPIb (Takamatsu et al., 2005). Once engaged with the streptococci the platelets become activated, spread, aggregate, and initiate thrombus formation, under which conditions, the bacteria are well protected from host immune defences and antibiotics (Jenne & Kubes, 2015; Jung et al., 2015).

The mechanisms by which platelets are activated by streptococci following adhesion are poorly understood. Recent work has identified the importance of specific antibodies in bacterial activation of platelets through receptor FcγRIIa (Arman et al., 2014; Pampolina & McNicol, 2005; Tilley et al., 2013). In *S. gordonii*, a ubiquitous human oral bacterium, there is direct activation of FcγRIIa integrin (non-antibody mediated), and then inside-out activation of the most highly-expressed platelet receptor GPIIb/IIIa (α_{IIb}β₃) (Keane et al., 2010). Further activation is associated with secretion of granules and secondary mediators,

[†]UCL Eastman Dental Institute, 256 Gray's Inn Rd, London WC1X 8LD.

filopodia formation (spreading), generation of ADP and thromboxane A₂ (TxA₂) to reinforce $\alpha_{IIb}\beta_3$ activation (Cox, Kerrigan, & Watson, 2011), and then aggregation with nearby-activated platelets via fibrinogen (Moriarty et al., 2015).

We have identified a protein designated Platelet adherence protein A (PadA), that is expressed on the surface of *S. gordonii*, and which interacts directly with platelets (Petersen et al., 2010). PadA precursor (3,646 amino acid [aa] residues) comprises a N-terminal region of 1,328 aa residues containing a von Willebrand Factor (vWF)-like domain (aa residues 72–229), and a C-terminal region comprising 14 blocks of aa residue repeats (Petersen et al., 2010) with a bacterial cell wall anchor region and sortase (LPxTG) motif (Mazmanian, Ton-That, & Schneewind, 2001) (see Figure 1). PadA, unlike Hsa, does not interact with sialylated GPIb (Petersen et al., 2010), but was shown to bind directly to the platelet receptor $\alpha_{IIb}\beta_3$ over-expressed on the surface of Chinese hamster ovary cells (Petersen et al., 2010). Binding of PadA to $\alpha_{IIb}\beta_3$ on platelets results in platelet activation; however, it is not known if PadA is able to activate platelets on its own, or if it requires a coactivator. Previous results suggest that $\alpha_{IIb}\beta_3$ may bind to *S. gordonii* via common integrin-recognition motifs (RGT and AGD) present within the N-terminal region of PadA (Keane et al., 2013). Recently, it has emerged that another motif, NGR (Asn-Gly-Arg), found in the D domain of fibrinogen on each of the β and γ chains, plays an important role in the interaction of $\alpha_{IIb}\beta_3$ with fibrinogen (Moriarty et al., 2015). A similar motif is found within the N-terminal region of PadA, raising the possibility that this might be a key factor in recognition of $\alpha_{IIb}\beta_3$ by PadA.

In this article, we have investigated the relative functions of Hsa and PadA in *S. gordonii* platelet interactions, and in bacterial cell binding to various extracellular matrix components that may be exposed at sites of endothelial damage, for example, fibronectin or vitronectin. We have also studied in more detail the interactions of the mature N-terminal F2 region (657 aa residues) of PadA with platelets and matrix components, and more specifically the relative

roles of the integrin-recognition motifs and NGR in *S. gordonii* host interactions.

2 | RESULTS

2.1 | Expression of *padA* and *hsa* in deletion mutants and complemented strains

A diagrammatic representation of PadA protein is presented in Figure 1 together with a visual expansion of the 690 aa-residue precursor N-terminal domain (F2) of main focus in this paper, and the corresponding aa sequence. Three integrin-like recognition motifs within the F2 domain are highlighted. To investigate further the functional properties of the PadA protein, the entire coding region was cloned into replicative plasmid vector pMSP downstream of a nisin-inducible promoter (see 4). The *hsa* gene was cloned in the same way as previously described (Jakubovics, Brittan, Dutton, & Jenkinson, 2009). Because Hsa is glycosylated by various products encoded by genes within the *hsa*-accessory secretion system locus (Zhou & Wu, 2009), authentic Hsa protein has not been expressed in a surrogate host bacterium. The results obtained from PadA Western immunoblot analyses of mutant and complemented strains are shown in Figure 2a. PadA protein was deficient in cell wall extracts of the $\Delta padA$ and $\Delta padA \Delta hsa$ mutants, and was highly-expressed in the complemented strains following 10 ng nisin ml⁻¹ induction. Hsa production was detected with succinylated-wheat germ agglutinin (sWGA), which recognizes the glycosylated protein (Takahashi, Yajima, Cisar, & Konishi, 2004). Hsa was well-expressed ectopically in the complemented Δhsa and $\Delta padA \Delta hsa$ mutants when induced with 50 ng nisin ml⁻¹ (Figure 2b,c). Higher nisin concentrations were growth-inhibitory. Production of Hsa from the chromosomal locus in the $\Delta padA$ mutant was unaffected and was similar to wild type strain DL1 expression levels (Figure 2c; Petersen et al., 2010).

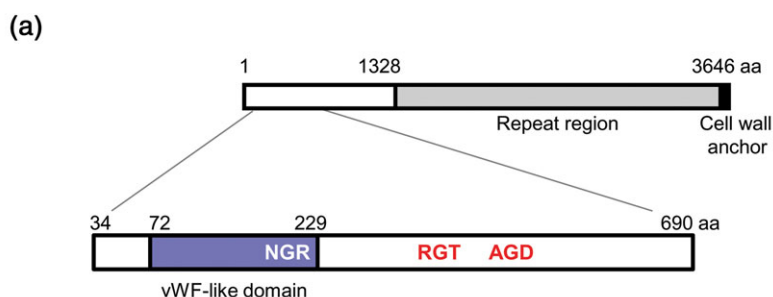


FIGURE 1 Diagrammatic representation of PadA protein and N-terminal F2 domain. (a) PadA precursor comprises 3,646 aa residues with N-terminal region (1,328 aa), and C-terminal region (2,318 aa) carrying 14 repeat blocks of 148–152 aa residues and a cell wall anchor motif LPKTG. The F2 region of the PadA polypeptide (657 aa) has been expanded to show the extent of the vWF-like domain and the approximate positions of NGR, RGT, and AGD motifs. (b) aa sequence of the N-terminal region 690 aa residues, indicating signal (leader) sequence (in green), the vWF-like domain (purple), and the three integrin-recognition motifs, NGR (214–6 aa), RGT (416–8 aa), and AGD (485–7 aa) in red type

1 MKDFLKVKVILFTVLLMSMPSSVNLGTSVVRADDP LNIETRRIDEHTTITQNGCYRKIE
61 KTDATDWTVPKPIDLVILQDASGSFRITIPSVKNALKRLTTYVSPEQYDENDPHLVKTD
121 DPRTTDRVFVASYQGLDQVRYFENNDFFSGNPANVYTDANSTGKNYTYGNSGLTSDQNKVH
181 NPIDNIAVDGGTPTVPAIDDTIAQYNRVKGNMENGRTKTVFLLVTDGVANGYRLPGTNTVV
241 MDKSWTRTDAIQKAWRVDSYPEAAQDIIGRANELKAAGNQLKAAVSGSVVVGFWERVD
301 NFTEKYYQYGPAYLNGFGNTINIGDNRVQAIIFHDALQSMASPKVNVGNKNSFYVNEQN
361 NIDVFSQKILESVAALVKDDITGEFDITEGYKVDAIRINGKKIIPKVTDPSKEIRGTIT
421 QTGNKVKISVPDSVFNPGKNSFDYLSKEARAPETDEDEVDPPENYVPEKEEITVPELT
481 GKFKAGDFETRIQGRNQTVVEQKLEYCPSATKTVKDADASNDIGVIPDPLELTKKPSY
541 SAQLSKKDEEFTYTVDYNNFNNVPEFEKNVMLTDPIDYRLEVVSASHAQGPDGQSWPTRVV
601 TQQDAGNSQSVVADVPPQGDYNYLIMKKAKLKMTVRLKEEYRKNQASKAYLAILQNN
661 NGYGLVNQGNIMWNGEDDSPNQDAHAKTKD₆₉₀

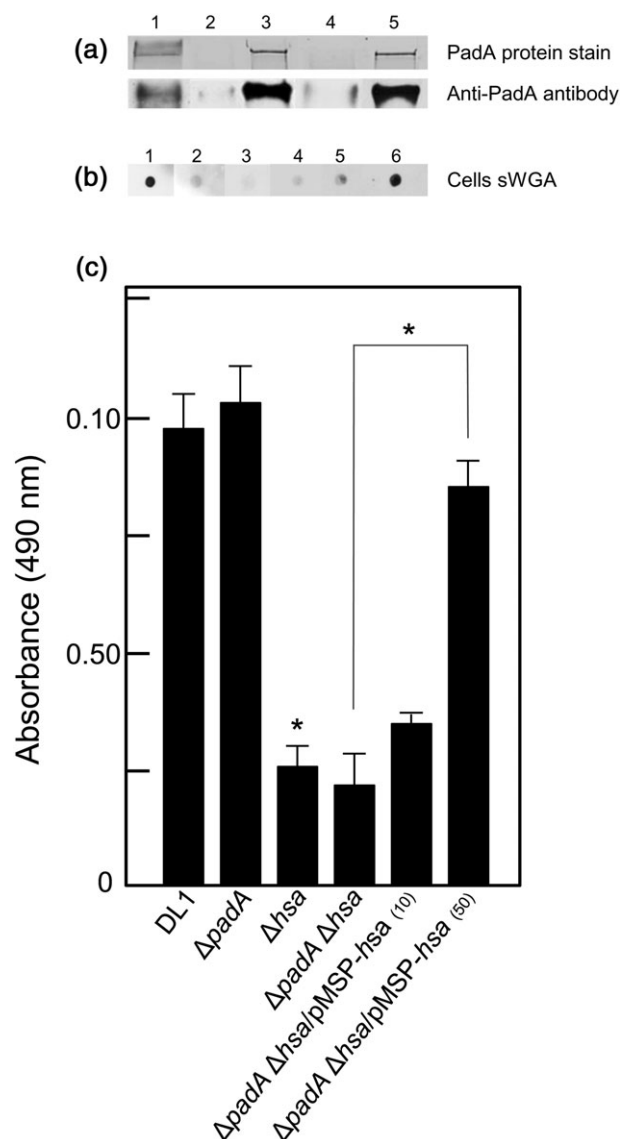


FIGURE 2 Expression of PadA and Hsa proteins by *S. gordonii* DL1 wild type, mutants and complemented mutants. (a) (composite), SDS-PAGE gel, and corresponding Western immunoblot of PadA (~350 kDa) in cell wall proteins extracted from: (1) DL1; (2) UB2723 $\Delta padA$; (3) UB2724 $\Delta padA$ /pMSP-*padA*; (4) UB2773 $\Delta padA$ Δhsa ; and (5) UB2775 $\Delta padA$ Δhsa /pMSP-*padA*. In lanes 3 and 5, protein expression was induced with 10 ng nisin ml⁻¹. (b) (composite), whole cell dot blots reacted with sWGA of: (1) DL1; (2) UB2029 Δhsa ; (3) UB2773 $\Delta padA$ Δhsa ; (4) UB2777 $\Delta padA$ Δhsa /pMSP-*hsa*; (5) UB2777 + 10 ng nisin ml⁻¹; and (6) UB2777 + 50 ng nisin ml⁻¹. (c) Biotinylated sWGA binding to immobilized bacterial cells (2×10^7 per well) followed by HRP-streptavidin to detect Hsa as described in 4. Figures in parentheses indicate ng ml⁻¹ nisin added to cultures to induce expression of Hsa in the complemented strain UB2777 $\Delta padA$ Δhsa /pMSP-*hsa*. Error bars represent ±SEM from two independent experiments ($n = 2$). * $P < 0.05$

2.2 | Role of PadA and Hsa in platelet adhesion by *S. gordonii*

It is well documented that Hsa interacts with platelets (Keane et al., 2010; Kerrigan et al., 2007; Takahashi et al., 2004), and we have previously shown that PadA also is involved in *S. gordonii* binding platelets (Petersen et al., 2010). This is confirmed (Figure 3) with the $\Delta padA$

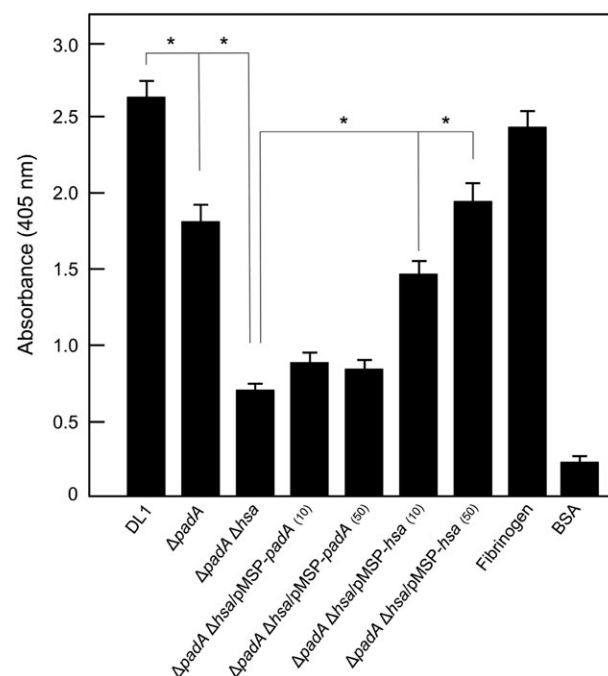


FIGURE 3 Platelet adhesion to immobilized *S. gordonii* strains under static conditions. Bacterial cells were deposited onto microwells, and platelet binding was determined by phosphatase assay as described in 4. Figures in parentheses indicate ng ml⁻¹ nisin added to cultures to induce expression of PadA or Hsa in the complemented strains UB2775 $\Delta padA$ Δhsa /pMSP-*padA*, and UB2777 $\Delta padA$ Δhsa /pMSP-*hsa*. Fibrinogen 100 μ g ml⁻¹ positive control; BSA 100 μ g ml⁻¹ negative control. Error bars represent ±SEM from four independent experiments ($n = 4$). * $P < 0.05$

mutant being approximately 30% reduced in levels of platelet adherence, and the $\Delta padA$ Δhsa mutant >80% reduced in binding platelets. Expression of *padA* in the $\Delta padA$ Δhsa mutant does not restore any level of platelet adhesion, but expression of *hsa* restored platelet binding levels to ~70% of wild type (Figure 3). These results show that interaction of PadA with resting platelets requires the presence of Hsa.

2.3 | PadA integrin-recognition motifs are essential for binding platelets

The above results suggest that Hsa and PadA might participate in a two-step reaction with platelets. We envisage that Hsa interacts with GPIIb (Bensing et al., 2004) resulting in inside-out signalling, activation of $\alpha_{IIb}\beta_3$, and PadA interacting with activated $\alpha_{IIb}\beta_3$ (Keane et al., 2013). In support of this hypothesis, a *padA* mutant was unaffected in binding purified $\alpha_{IIb}\beta_3$ but was abrogated in binding $\alpha_{IIb}\beta_3$ on the surface of Chinese hamster ovary cells (Petersen et al., 2010). The purified PadA-F2 fragment (Figure 1) binds weakly to non-activated platelets (Figure 4a) but at high levels to TRAP-activated platelets (Figure 4b). We were interested in determining the role of the NGR motif within PadA-F2 region because this same motif is present in fibrinogen and has been shown to interact with $\alpha_{IIb}\beta_3$ and activate platelets (Moriarty et al., 2015). Alanine substitutions of integrin-like recognition motifs NGR, RGT, or AGD, to AAA in each case, individually had no significant effects on binding of F2 fragment to activated platelets (Figure 4b). However, when all three motifs were substituted,

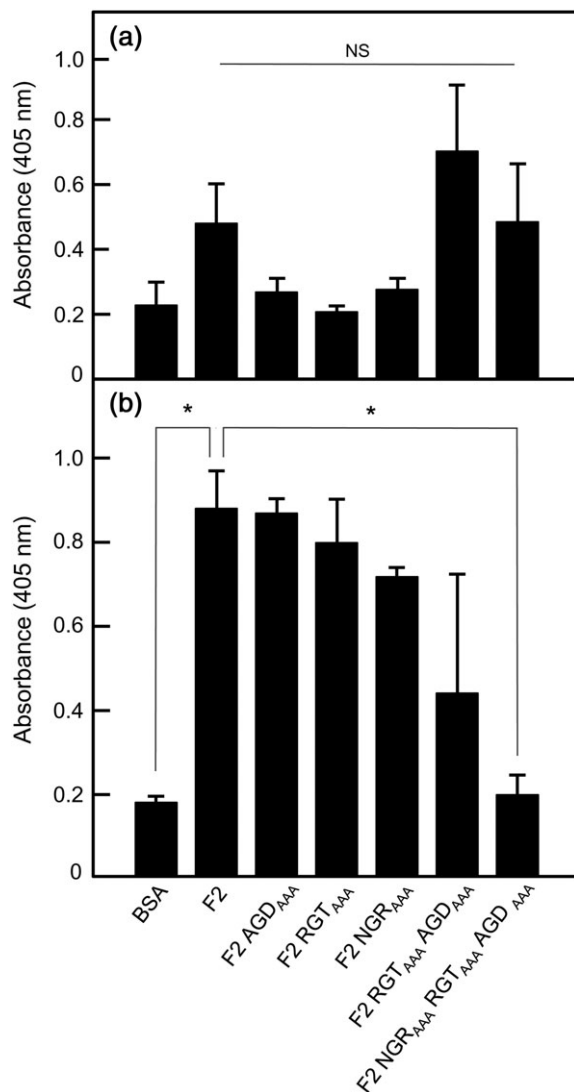


FIGURE 4 Adhesion of non-activated or TRAP-activated platelets to immobilized recombinant PadA-F2 region fragments under static conditions. Recombinant PadA protein fragments were immobilized onto microtitre plate wells (10 μ g per well), and non-specific binding sites were blocked with BSA. Gel-filtered platelets were either non-activated (a) or activated by addition of TRAP (Thrombin Receptor Activating Peptide; b) and were incubated with the immobilized proteins at 37°C for 45 min (2×10^7 platelets per well). Platelet adherence was determined by phosphatase assay. RGT_{AAA}, AGD_{AAA}, NGR_{AAA}, and so forth indicate the motifs within the various F2 fragments that were alanine-substituted to AAA. Error bars represent \pm SEM from three independent experiments ($n = 3$). * $P < 0.05$. In (a), NS = not statistically significant (F2 v F2 RGT_{AAA} AGD_{AAA}, $P = 0.429$; F2 v F2 NGR_{AAA} RGT_{AAA} AGD_{AAA}, $P = 0.962$)

activated platelet binding was abrogated (Figure 4b) while non-activated platelet binding was not significantly different from F2 (Figure 4a). Therefore, NGR is not only essential for interaction of PadA with activated platelets but also requires functional AGD and RGT motifs (Figure 4b).

Previously, we have suggested that the RGT and AGD motifs have little or no role in supporting platelet adhesion, but are involved in the transformation of the platelet biconcave disc through formation of filopodia and lamellipodia to a fully spread cell

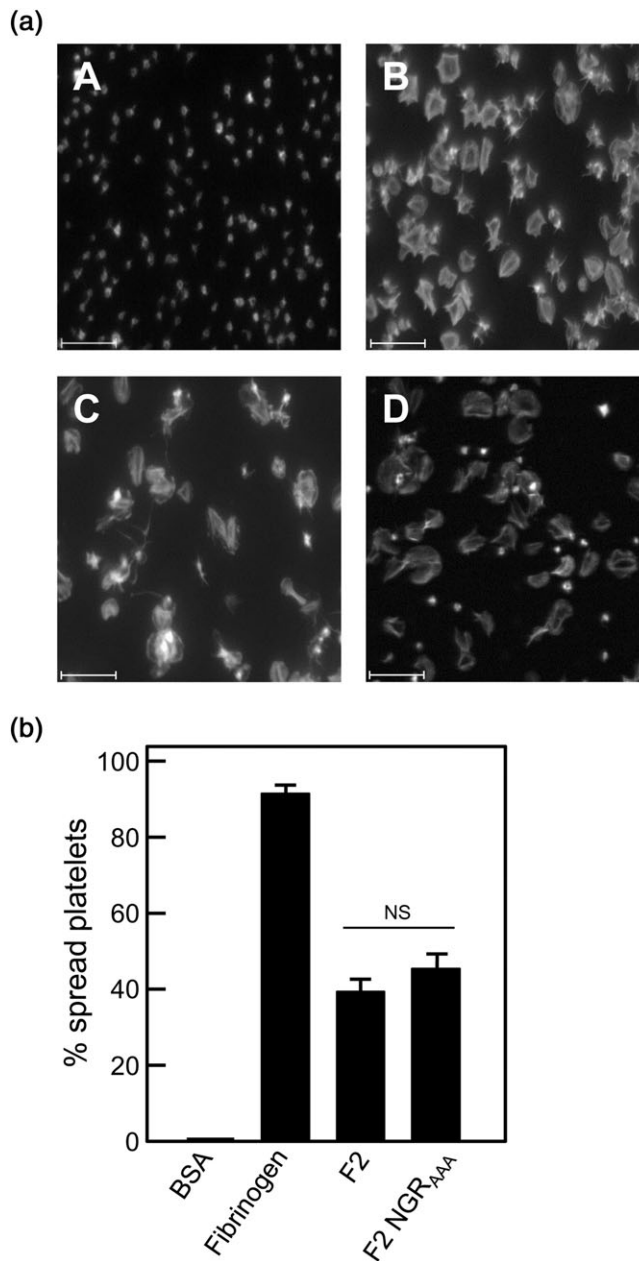


FIGURE 5 Platelet spreading on immobilized recombinant PadA-F2 region fragments under static conditions. (a) BSA (negative control), (b) fibrinogen (positive control), (c) recombinant PadA protein fragment F2, or (d) fragment F2 NGR_{AAA} were immobilized onto microtitre plate wells (10 μ g per well), and non-specific binding sites were blocked with BSA. Gel-filtered platelets were incubated with the immobilized substrates at 37°C for 45 min (2×10^7 platelets per well), and platelet spreading was visualized by confocal microscopy. Scale bar = 15 μ m. (b) Percentage of platelets spread on BSA (negative control), fibrinogen (positive control), and recombinant PadA protein F2 fragments immobilized onto glass slides. Error bars represent \pm SEM from three independent experiments ($n = 3$). NS = not statistically significant

(Keane et al., 2013). Accordingly, we tested the effect of NGR_{AAA} mutation on platelet spreading and found that for those platelets that adhered, spreading was unaffected (Figure 5). Taken collectively, these results suggest that NGR plays a major role in directing adhesion of platelets, while AGD and RGT promote spreading.

2.4 | Functions of PadA and Hsa in binding fibronectin

We then utilized an affinity chromatography proteomics approach to determine if PadA interacted with specific host proteins present in human plasma. Purified PadA protein with a $\times 6$ His C-terminal tag (PadA_{6His}) was linked to Ni-NTA magnetic beads and incubated with plasma. The beads were collected, washed, and the interacting proteins were eluted, subjected to SDS-PAGE, in-gel digested with trypsin, and analysed by tandem mass spectrometry. Data analysis (see 4) identified Fn1 protein (fibronectin) (B7ZLE5_HUMAN) as the highest scoring protein to be pulled down (99% identity confidence/ SEQUEST, 31.16% sequence coverage, 48 unique peptides) relative to plasma controls. Also, uncharacterized protein Q6GMX0_HUMAN was identified (47% sequence coverage, 1 unique peptide), recently annotated as anti-polyhydroxybutyrate antibody Fv light chain, the significance of which is unclear. Fibronectin and Q6GMX0 peptides were low scoring or non-detectable, respectively, in parallel plasma controls.

Fibronectin is an extracellular matrix (ECM) protein often found at sites of endothelial cell damage to which platelets and bacteria are attracted. Plasma fibronectin (pFn) is a major component of the fibrin clot (early wound repair), while cellular fibronectin is involved in later repair events (To & Midwood, 2011). It is known that Hsa is involved in *S. gordonii* binding to pFn by recognition of sialylated regions on the molecule (Jakubovics et al., 2009). Accordingly, we tested the $\Delta padA$ or Δhsa mutants and complemented strains in adherence to pFn and to cFn. Levels of binding were slightly higher to cFn, but the overall adherence patterns of the strains were identical; therefore, we only present the data for binding to cFn. The $\Delta padA$ mutant was approximately 25% reduced in binding cFn, while the complemented strain was above wild type levels of binding (Figure 6). These adherence events were reduced by 50–60% when the cFn was desialylated (Figure 6). Deletion of *hsa* led to ablation of cFn binding, while complementation of the Δhsa mutant led to part-restoration of cFn-binding activity (Figure 6). Complementation of the $\Delta padA \Delta hsa$ mutant with *padA* led to a small increase in cFn binding, while complementation with *hsa* restored binding levels to just below wild type (Figure 6). We therefore conclude that Hsa is a major mediator of Fn binding under these conditions and that PadA plays a minor, but significant, role in the process. The fact that adhesion levels are only 50–60% reduced for desialylated cFn is consistent with the presence of PadA and other proteins that interact with non-sialylated Fn (Jakubovics et al., 2009).

2.5 | Functions of PadA and Hsa in binding vitronectin

Vitronectin (Vn) is a component of the α -granules of platelets as well as being found in ECM where it regulates proteolysis, promotes cell adhesion and spreading, and modulates the activities of components of the complement pathway (Singh, Su, & Riesbeck, 2010). Bacteria coated with Vn evade complement assault, and Vn cross-links bacteria and host cells, thence triggering host cell signalling and cytoskeletal remodelling (Singh et al., 2010). Accordingly, we also determined the role of PadA and Hsa in binding to Vn. Deletion of *padA* resulted in

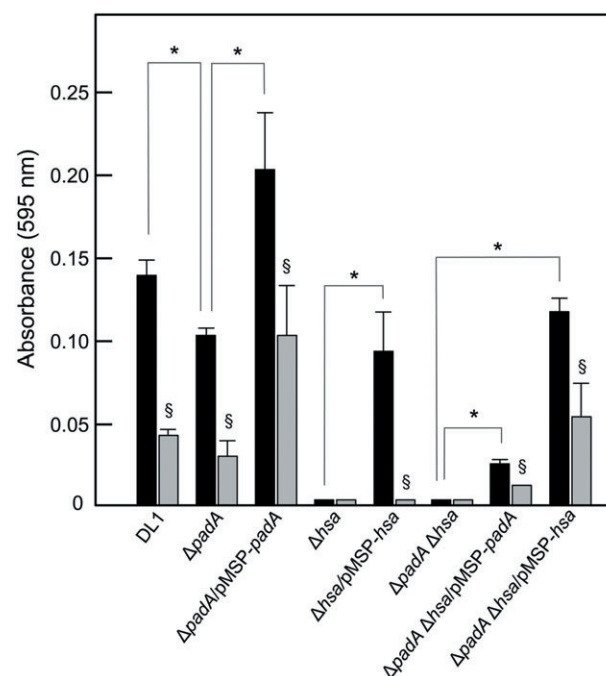


FIGURE 6 Adhesion of *S. gordonii* strains to human cellular fibronectin (cFn). Microtitre plate wells were coated with cFn (1 μ g per well), blocked with BSA, and then incubated with streptococcal cells (5×10^7 per well) for 2 hr at 37°C. Bacterial cells adhered (black columns) were quantified by staining with crystal violet as described in 4. Wells coated with cFn were also incubated with 0.001 U neuraminidase (sialidase) for 2 hr at 37°C, washed, blocked with BSA and then incubated with streptococcal cells (grey shaded columns). Expression of PadA or Hsa proteins by complemented strains was induced with 10 ng or 50 ng nisin ml^{-1} . Error bars represent \pm SEM from three independent experiments ($n = 3$). * $P < 0.05$ for comparisons indicated; \$ $P < 0.05$ for neuraminidase-treated cFn versus untreated

60% reduction in Vn-binding levels (Figure 7) while adherence was fully restored by complementation with *padA* (Figure 7). Deletion of *hsa* abrogated binding of mutant cells to Vn, and complementation with ectopic *hsa* restored binding to about 45% of wild type levels. Interestingly, complementation of $\Delta padA \Delta hsa$ with either *padA* or *hsa* alone did not complement the Vn-binding phenotype. These results strongly indicate that Hsa requires the presence of functional PadA in order to efficiently bind Vn. Lastly, adherence of streptococcal cells to Vn was ablated by sialidase (neuraminidase) treatment of Vn, implying that Vn adherence is sialylation dependent (Figure 7).

2.6 | Functions of PadA and Hsa in adherence to salivary glycoproteins and in biofilm formation

S. gordonii is normally found in the oral cavity and produces a spectrum of adhesins that interact with salivary components (Nobbs, Lamont, & Jenkinson, 2009). To test the effects of *padA* or *hsa* deletions on initial streptococcal adherence to salivary pellicle, bacteria were incubated with saliva-coated glass cover slips, and levels of adhesion determined by crystal violet staining. We detected significant differences in adherence of the $\Delta padA$ and $\Delta padA \Delta hsa$ mutants compared with wild type DL1 (Figure 8). Complementation with *padA* restored adherence levels while complementation with *hsa* did not (Figure 8).

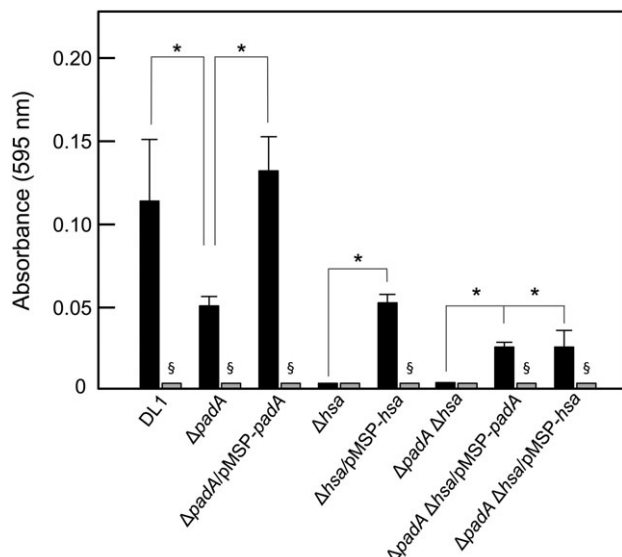


FIGURE 7 Adhesion of *S. gordonii* strains to human vitronectin (Vn). Microtitre plate wells were coated with Vn (0.05 μg per well), blocked with BSA, and then incubated with streptococcal cells (5×10^7 per well) for 2 hr at 37°C. Bacterial cells adhered (black columns) were quantified by staining with crystal violet as described in 4. Wells coated with Vn were also incubated with 0.001 U neuraminidase (sialidase) for 2 hr at 37°C, washed, blocked with BSA, and then incubated with streptococcal cells (grey columns). Expression of PadA or Hsa proteins by complemented strains was induced with 10 ng or 50 ng nisin ml^{-1} , respectively. Error bars represent $\pm\text{SEM}$ from three independent experiments ($n = 3$). * $P < 0.05$ for comparisons indicated; § $P < 0.05$ for neuraminidase-treated Vn versus untreated

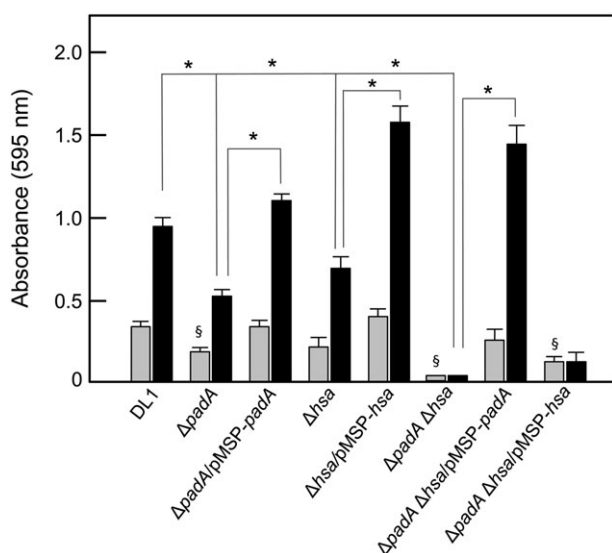


FIGURE 8 *S. gordonii* strains adherence to salivary pellicle and biofilm formation. Cover slips were coated with salivary pellicle and incubated with streptococcal cells (5×10^7 per well) for 2 hr at 37°C for adherence (grey columns) or in YPT-Glc medium for 16 hr at 37°C for biofilm formation (black columns). Bacterial cells adhered, and biofilm biomass values were quantified by staining with crystal violet as described in 4. Expression of PadA or Hsa proteins by complemented strains was induced with 10 ng or 50 ng nisin ml^{-1} , respectively. Error bars represent $\pm\text{SEM}$ from three independent experiments ($n = 3$). * $P < 0.05$ for biofilm comparisons indicated; § $P < 0.05$ for significantly different adherence versus DL1

In subsequent biofilm formation, the ΔpadA mutant was 50% decreased in biomass compared to wild type, and complementation with *padA* restored biomass to slightly above wild type levels (Figure 8). Deletion of *hsa* resulted in similar effects, and complementation of the Δhsa mutant was highly effective in enhancing biofilm formation. The $\Delta\text{padA} \Delta\text{hsa}$ mutant was ablated in biofilm formation (Figure 8). Complementation with *padA* restored biofilm formation, but complementation with *hsa* did not (Figure 8). These results suggest that PadA must be fully functional for Hsa to promote biofilm formation. However, it also appears that PadA alone can provide the necessary function for biofilm formation in the absence of Hsa (Figure 8).

2.7 | PadA integrin-recognition motifs are not involved in binding cFn, Vn, or salivary pellicle

Because the previous data strongly suggest that PadA is involved in binding ECM substrata and salivary pellicle, we tested the ability of the PadA-F2 region to mediate these interactions, and the role of the three integrin-recognition motifs. In binding assays of purified F2 fragments to immobilized substrata, it was found that levels of binding to cFn were higher than to Vn and pellicle (Figure 9). Substitution of all three integrin-recognition motifs (RGT, AGD, and NGR) with AAA failed to significantly affect levels of adhesion of the PadA-F2 fragment to Fn, but there was slightly elevated interaction with Vn and with salivary pellicle (Figure 9). Sialidase treatment of the substrata did not affect levels of PadA-F2 binding compared to untreated substrata (Figure 9).

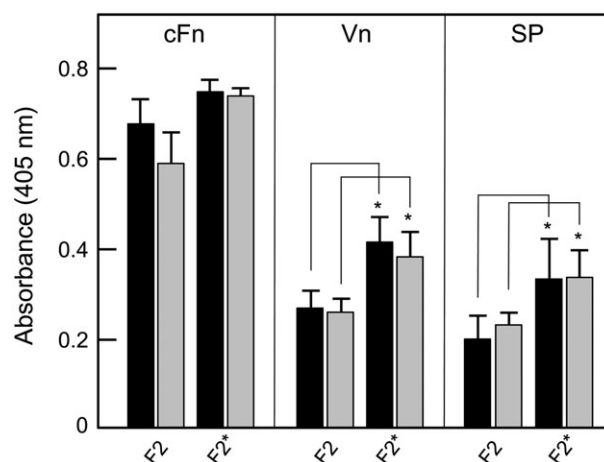


FIGURE 9 Adhesion of PadA-F2 region fragments to cellular fibronectin (cFn), vitronectin (Vn), or salivary pellicle (SP). cFn, Vn, or saliva were immobilized onto microtitre plate wells and non-specific binding sites were blocked with BSA (black columns). Wells coated with cFn, Vn, or salivary glycoproteins were also incubated with 0.001 U neuraminidase (sialidase) for 2 hr at 37°C, washed, and blocked with BSA (grey columns). Recombinant proteins (100 μg ml^{-1}) were incubated with substrata for 2 hr at 37°C and amounts bound measured with anti-tetra-His mouse antibodies and HRP-conjugated anti-mouse IgG antibodies as described in 4. F2, unmodified fragment; F2*, fragment containing NGR, RGT, and AGD motifs all alanine-substituted to AAA. Error bars represent $\pm\text{SEM}$ from three independent experiments ($n = 3$). * $P < 0.05$ compared with corresponding F2 values

3 | DISCUSSION

S. gordonii is a component of the normal microbiota of the human oral cavity and plays a pivotal role in the development of microbial communities on the tooth surfaces and gingival crevices (Jenkinson, 2011; Wright et al., 2013). These communities provide a reservoir for bacteria to enter the circulation where they may interact with blood platelets and cause unwanted thrombus generation. This can lead to infective endocarditis, which is characterized by the formation of vegetations on the heart valves (Moreillon & Que, 2004). Significant advances in our understanding of how *S. gordonii*, and other mitis-group oral bacteria, interact with platelets have been made in recent years.

In addition to the knowledge about *S. gordonii* Hsa and GspB proteins (Takahashi et al., 2002; Xiong, Bensing, Bayer, Chambers, & Sullam, 2008), and how they are able to interact with platelet integrin GPIb (Takamatsu et al., 2005), we have demonstrated that PadA surface protein can bind to platelets in a $\alpha_{IIb}\beta_3$ -dependent manner (Petersen et al., 2010) causing dense granule secretion and full platelet spreading (Keane et al., 2010). The N-terminal region of 1328 aa residues interacts with platelets (Keane et al., 2013; Petersen et al., 2010), and here, we show that the same region binds Vn, Fn, and salivary pellicle. The PadA C-terminal region comprising 2,318 aa residues has no defined function at this stage. It is thought that this region containing aa residue repeat blocks (Figure 1) may act as a flexible stalk holding the N-terminal binding-region of the protein out into the environment. C-terminal region repeat-block regions of other *S. gordonii* surface proteins, such as CshA and Hsa, are reported to provide extended conformations (McNab et al., 1999; Takahashi et al., 2002) that may assist in capture of their ligands even under conditions of shear or flow (Kerrigan et al., 2007).

In the first part of the present study, we focused on the roles of three integrin-like recognition motifs within the N-terminal PadA-F2 fragment (657 aa residues) in the interactions of PadA with platelets. We showed previously that neither RGT_(416–418) nor AGD_(485–487) were necessary for supporting static or shear-induced platelet adhesion, but both motifs contributed to platelet spreading (Keane et al., 2013). This is in keeping with the data suggesting that Hsa is essential for platelet capture under shear and thus responsible for platelet rolling (Bensing et al., 2004; Kerrigan et al., 2007). Firm adhesion is then complete when platelet integrin $\alpha_{IIb}\beta_3$ interacts with PadA (Petersen et al., 2010). Recent evidence indicates that another motif, NGR, within fibrinogen is responsible for interaction with $\alpha_{IIb}\beta_3$ and triggering platelet activation (Moriarty et al., 2015). In light of this discovery, we investigated the role of an identical motif NGR_(214–216) within the N-terminal region of PadA to direct interactions with platelets. In our experiments with platelets that were specifically in resting state, we found that the PadA-F2 fragment bound these only weakly (Figure 4a). However, the immobilized PadA-F2 region bound TRAP-activated platelets, so this would be in keeping with the notion that PadA preferentially interacts with $\alpha_{IIb}\beta_3$ that is in an activated complex with GPIb following Hsa-binding. Confirming our previous studies, we showed that RGT and AGD were not essential for PadA-F2 binding to TRAP-activated platelets. However, binding of the PadA-F2 fragment to activated platelets required the combined

activities of NGR, RGT, and AGD, because alanine-substitutions of all of these motifs ablated adhesion (Figure 4b). Moreover, we could not demonstrate that the NGR motif alone was necessary for full platelet spreading, while RGT and AGD motifs clearly contribute to the full spreading process (Keane et al., 2013). In summary, we are nearing the situation in which we could potentially target these three motifs within PadA as a means to controlling unwanted platelet activation by circulating *S. gordonii*, and by other oral streptococci that express PadA-like proteins.

In this study, we have also utilized gene knockouts and respective complemented strains of *S. gordonii* in order to dissect the relative functions of PadA and Hsa in host tissue interactions. Our results have uncovered some unexpected dependencies of the two proteins on each other for their adhesive functions. Platelet adhesion depends upon the dual functioning of Hsa and PadA, as previously interpreted, but knock-in of PadA to a $\Delta padA \Delta hsa$ double mutant does not restore adhesion, only knock-in of Hsa part-restores adhesion. This appears to support evidence that PadA contributes to adhesion only when platelets have first been engaged with Hsa. The fact that knock-in of Hsa does not fully restore platelet adhesion shows the requirement of PadA for complete engagement (Figure 3).

Our experiments with *S. gordonii* mutants also demonstrate that PadA and Hsa are involved in binding Fn and Vn. Binding of *S. gordonii* to cFn is in part sensitive to sialidase treatment of cFn, and this is consistent with the known activity of Hsa in Fn-binding by *S. gordonii* (Jakubovics et al., 2009). It is possible that regions outside the Siglec-like sialic acid-binding domain within the BR (binding region) of Hsa (Pyburn et al., 2011) interact with Fn. For example, the BRs of *Streptococcus agalactiae* serine-rich repeat proteins Srr1 and Srr2 have been shown to bind fibrinogen (Seo et al., 2013). Another *S. gordonii* surface protein that interacts with Fn is CshA (McNab et al., 1999). Neither CshA nor PadA contain primary sequences or motifs that have been associated with Fn recognition by other Gram-positive bacterial cell surface proteins (Henderson, Nair, Pallas, & Williams, 2011). The mechanism of cFn binding by PadA is currently under investigation. In summary, Hsa is a major component of the *S. gordonii* cell surface that binds sialylated Fn. PadA also binds cFn, but this is less effective in the absence of Hsa (Figure 6) suggesting that, like for platelets, Hsa binding sialic acid residues promotes PadA function.

The finding that $\Delta padA$ and Δhsa mutants of *S. gordonii* are also deficient in binding to Vn may have significance in the overall processes of platelet binding and activation, and in immune evasion. Vn is present in plasma, ECM and in platelet α -granules. Blood platelets secrete multimeric Vn following activation, although about 50% remains platelet bound (Parker, Stone, White, & Seinschaw, 1989). Vn forms complexes with plasminogen activator inhibitor-1 (PAI-1) and thus behaves as a physiological inhibitor of active thrombin. Conversely, Vn also appears to stabilize the thrombus and, so, plays a dual role in mediating platelet adhesion (Thiagarajan & Kelly, 1988) and aggregation (Reheman et al., 2005). Vn carries binding sites for heparin, PAI-1, integrins, collagen and plasminogen (Ekmekçi & Ekmekçi, 2006) and also binds $\alpha_{IIb}\beta_3$. Thus, *S. gordonii* might be able to interact with platelets via Vn, which may be bound to β_3 integrins or to surface-associated collagen. Furthermore, bacteria coated with Vn are able to evade the membrane attack complex (MAC) by blocking complement

Experiments investigating adherence to salivary pellicle and biofilm formation set out to determine if there were roles for the PadA and Hsa proteins in oral cavity colonization outside of pathogenesis within the circulatory system. It is already known that Hsa and GspB bind salivary proteins (Takamatsu, Bensing, Prakobphol, Fisher, & Sullam, 2006), and that Hsa is required for intergeneric coaggregation with *Veillonella* species (Zhou, Liu, Li, Takahaski, & Qi, 2015). However, this is not sialic acid-dependent, providing further evidence for the presence of additional binding sites within the BR of Hsa. The ability

of *S. gordonii* to adhere to pellicle is antecedent to biofilm formation. Both PadA and Hsa appear to contribute to biofilm formation and complementation of $\Delta padA$ or Δhsa single knock-out mutants restores the ability to form biofilms in each case. However, only complementation of the $\Delta padA \Delta hsa$ mutant with PadA restored biofilm formation, not complementation with Hsa. We conclude with an important interpretation that the role of Hsa in biofilm formation is only effective in the presence of PadA. Clearly, therefore, PadA has the ability to mediate *S. gordonii* binding to salivary pellicle in the absence of sialic acid receptors (Figure 9), and to promote cell-cell interactions that also do not involve sialic acid receptors and result in biofilm formation. This could mean that biofilm formation is a two-step process, and that PadA provides the first step (as opposed to the secondary step in binding platelets). Alternatively, Hsa and PadA may independently contribute to biofilm formation but Hsa is not functionally expressed without the presence of PadA. This might suggest that a complex is formed between PadA and Hsa on the *S. gordonii* cell surface, and this possibility is currently under investigation.

In conclusion, PadA is a multi-domain adhesin that interacts with activated platelets via $\alpha_{IIb}\beta_3$ facilitating firm adhesion, granule release, and full platelet spreading (see Figure 10). These properties depend upon the presence of NGR, RGT, and AGD integrin-like recognition motifs within the N-terminal F2 fragment of 657 aa residues. These motifs are not involved in PadA-F2 fragment binding to cFn, Vn, or salivary pellicle, suggesting that they are more critical to platelet interactions, and that the alanine substitutions did not significantly affect the general adhesion properties of the F2 region. PadA functions in concert with Hsa, mediating firm adhesion of platelets following

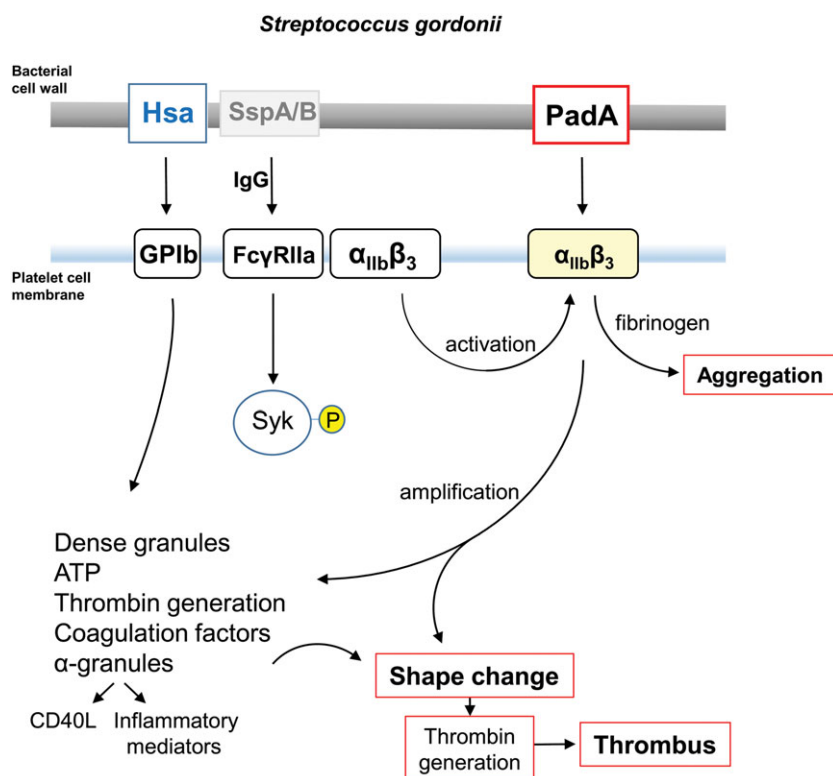


FIGURE 10 Diagrammatic representation of some of the processes involved in platelet activation by *S. gordonii*. Cell wall-anchored proteins Hsa and PadA interact with platelet membrane integrins GPIIb and $\alpha_{IIb}\beta_3$ (GPIIb/IIIa). Hsa captures platelets under flow (rolling) by binding GPIIb, and possibly also $\alpha_{IIb}\beta_3$, and activates signalling cascades including Fc γ R1a phosphorylation, leading to dense granule release (see Arman et al., 2014). PadA binds activated $\alpha_{IIb}\beta_3$, thus amplifying signals leading to shape change, thrombin production, coagulation, and thrombus formation. Platelet activation by *S. gordonii* can occur in the absence of specific IgG. However, with IgG present, there is evidence for activation (phosphorylation) of spleen tyrosine kinase (Syk-P) through Fc γ R1a. Conserved streptococcal surface protein antigens such as antigen I/II proteins (e.g., SspA/B) may also be involved in the overall process (Kerrigan et al., 2007). Physiologically, collagen activates Syk through GPVI, which is closely associated with Fc γ R1a (not shown). Fibrinogen engages GPIIb/IIIa ($\alpha_{IIb}\beta_3$), which also associates with Fc γ R1a. CD40L (otherwise known as CD154) is up-regulated in the platelet cell membrane and binds CD40⁺ cells such as endothelial cells and neutrophils, while soluble (released) CD40L further activates platelets

TABLE 1 List of primers. Restriction enzyme sites are underlined

Primer	Sequence
aad9.seqF	5' GGATACATTCTCAGAAGGAA 3'
padA.F1	5' <u>GGCTCGAGCGGA</u> ATTTAACTAGGAGGG 3'
padA.R1	5' CCTGGACGCGGCCCATGCTATTTTAAAGCCTATATAA 3'
padA.F2	5' TAGCATGGCGCCGTCAGGAGAGCTATGCTCTT 3'
padA.R2	5' TCCCCCGGGGTCGTAATCTCTGGTTGAGG 3'
aad9F.NarI	5' CGCGGCGCCGTAACGTGACTGGCAAG 3'
aad9R.NarI	5' CGCGGCGCCGATGCATATGCATGCTGC 3'
Terminator.XhoF	5' ATGATACATGCTCGAGGAATTAGGTTGAAAAATAGAAGG3'
Terminator.XhoR	5' GGAGACCGGCTCGACTGAACACAAAGCTCGTAAGATC 3'
padA.pMSPF	5' ATGATACATGCTCGAGGATTTTTTAAAAAGGTTTAAATAC 3'
padA.pMSPR	5' AACCTAATTCCTCGAGTTAATGCTTTGGTTTCTTCTC 3'
JH5F	5'PHO- GCTGCTGCAATCACACAGACCGGTAACAAGG 3'
JH6R	5'PHO-GATTTCTTGCTAGGGTCTGTTACTTTCGG 3'
JH19F	5'PHO- GCGGCCGCTAAGACGGTCTTCTCCTAGTAACGG 3'
JH20R	5' PHO - TTCCATATTCCTTTGACACGGTTGTAAGTACTGAGC 3'
His.padAR	5' ATGATGATGTGCTCCGTCTTAAATAGATG
His.padAF	5' CACCACCACTAACTCGAGGAATTAGGTTG

capture of platelets by Hsa via GPIb, and firm adhesion to cFn. PadA and Hsa also act cooperatively in mediating binding of bacteria to Vn, salivary pellicle, and biofilm formation. In the latter phenotype, Hsa is clearly reliant on PadA expression to mediate its function. Taken collectively, these results strongly suggest that in *S. gordonii* at least two cell wall-anchored proteins work in concert to mediate host-interactive processes relevant to both bacterial colonization and pathogenesis.

4 | EXPERIMENTAL PROCEDURES

4.1 | Bacterial growth conditions

Streptococcus gordonii DL1-Challis, isogenic mutants UB2723 $\Delta padA::aad9$, UB2029 $\Delta hsa::aphA3$, UB2773 $\Delta padA::aad9 \Delta hsa::aphA3$, and mutant strains complemented with pMSP-*padA* or pMSP-*hsa*, were routinely grown on BHY agar (37 g l⁻¹ Brain Heart Infusion, 5 g l⁻¹ Yeast Extract, 15 g l⁻¹ agar) or in BHY broth, at 37°C under CO₂-enriched conditions (candle jar). Less complex TY medium (5 g l⁻¹ Bacto-tryptone, 4 g l⁻¹ yeast extract, 4 g l⁻¹ K₂HPO₄, adjusted to pH 7.5 with HCl) containing 0.5% glucose (TY-Glc) was employed for protein purification from *S. gordonii* UB2870 $\Delta padA$ /pMSP-*padA*_{6His}. Protein expression from pMSP was under control of a nisin-inducible (10–50 ng ml⁻¹) promoter (Bryan, Bae, Kleerebezem, & Dunne, 2000; Hirt, Erlandsen, & Dunne, 2000). *Escherichia coli* strains DH5a, JM109, XL1-Blue, Stellar® and BL21 for plasmid preparation and protein expression were grown on LB agar or in LB broth at 37°C. Antibiotics were incorporated where necessary for streptococci [5 µg erythromycin (Em) ml⁻¹; 100 µg spectinomycin (Sp) ml⁻¹; 250 µg kanamycin (Kn) ml⁻¹] or *E. coli* [100 µg ampicillin (Ap) ml⁻¹; 250 µg Em ml⁻¹].

4.2 | Generation of *S. gordonii* gene knockout strains

Plasmids or PCR amplimers were purified using QIAquick Spin Miniprep or PCR Purification kits respectively (Qiagen, Manchester,

UK). Oligonucleotides (Table 1) were synthesised by MWG Eurofins (Wolverhampton, UK). Chromosomal DNA was extracted from mutanolysin-treated *S. gordonii* DL1 cells, as described previously (Jenkinson, 1987). DNA restriction and modification enzymes were used under the conditions specified by the manufacturer (New England Biolabs, Hitchin, Herts, UK).

The *padA* gene of *S. gordonii* DL1 was deleted by allelic exchange with the Sp resistance determinant *aad9*. PCR amplification using Expand Long PCR System (Roche, Burgess Hill, West Sussex, UK) with primers padA.F1/padA.R1 and padA.F2/padA.R2 and *S. gordonii* DL1 chromosomal DNA template generated two fragments comprising the flanking sequences of the *padA* gene (676 BP, 518 BP) with a unique NarI site at their 3' and 5' ends, respectively. These were stitched together in a second round of PCR using primers padA.F1/padA.R2 generating a 1155-bp amplimer with an internal unique NarI site. The fragment was subsequently cloned into pGEM-T Easy to generate construct pGEM-*padA*flank and transformed into chemically-induced competent cells (Hanahan, 1983) of *Escherichia coli* XL1-Blue. The *aad9* gene was PCR amplified from plasmid pFW5 (Podbielski, Spellerberg, Woischnik, Pohl, & Lütticken, 1996) using primers aad9F.NarI/aad9R.NarI and then sub-cloned into the NarI site of pGEM-*padA*flank to generate construct pGEM-*padA*flank::*aad9*. PCR amplification from pGEM-*padA*flank::*aad9* with primers padA.F1/padA.R2 generated amplimer *padA*flank::*aad9*, which was transformed into *S. gordonii* DL1 as described by Haisman and Jenkinson (1991) to produce the *padA* gene knockout mutant (designated UB2723). Confirmation of successful mutagenesis was obtained by sequencing the PCR product amplified from the chromosomal locus with primer pair padA.F1/padA.R2. Absence of PadA protein from the cell wall of the mutant was verified by Western immunoblotting using anti-PadA antibodies (Petersen et al., 2010).

To generate a *S. gordonii* DL1 $\Delta padA \Delta hsa$ double-knockout mutant, *S. gordonii* UB2029 $\Delta hsa::aphA3$, a reisolate of UB1545 (Jakubovics et al., 2005), was used as recipient for allelic replacement

of the *padA* gene with *aad9*. Primers *padA.F1/padA.R2* were utilized to amplify with PrimeSTAR Max polymerase (Takara Biotechnology, Shiga, Japan) a 2-kb fragment from UB2723 chromosomal DNA. The amplicon was purified and transformed into *S. gordonii* UB2029 with selection for Kn^R and Sp^R , and colonies were screened by PCR using primers *aad9.seqF/padA.R2* to detect the *aad9* cassette. Several transformants were checked by sequencing PCR products generated from across the loci and a representative transformant was purified and designated UB2773.

4.3 | Generation of *S. gordonii* complemented mutant strains

To complement the *S. gordonii* UB2723 $\Delta padA$ mutant, the entire *padA* coding sequence was cloned into pMSP, a derivative of pMSP7517 (Hirt et al., 2000) in which the *prgB* gene had been replaced by DNA encoding three alanine residues, together with the transcriptional terminator of the *padA* operon. In brief, a 227-bp region downstream of SGO_RS09805 incorporating the *padA* operon transcriptional terminator was amplified from *S. gordonii* DL1 chromosomal DNA using PrimeSTAR® GXL polymerase (Takara Biotechnology, Shiga, Japan) with primers Terminator.XhoF/Terminator.XhoR. The amplicon was cloned using In-Fusion HD Cloning Kit (Clontech, Oxford, UK) into vector pMSP, which had been linearized by digestion with XhoI. The primers were designed such that only the XhoI site at the 5' end of the transcriptional terminator would be retained upon cloning. This construct (pMSP-term) was transformed into *E. coli* K12 and confirmed by sequencing. The *padA* gene (10,967 bp) was then amplified using primers *padA.pMSPF/padA.pMSPR* and cloned via XhoI sites at its termini into pMSP-term that had been similarly digested. The resulting construct (pMSP-*padA*) was transformed into *E. coli* K12 and confirmed by sequencing. The construct was then transformed into *S. gordonii* UB2723 $\Delta padA$ and into UB2773 $\Delta padA \Delta hsa$ to generate complemented mutants. PadA expression was under control of the nisin-inducible promoter present in pMSP, and so following nisin induction ($10\text{--}50 \text{ ng ml}^{-1}$) PadA expression by the complemented strains was confirmed by Western immunoblot of cell wall protein extracts and whole cell FACS analyses, with anti-PadA antibodies (Figure 2).

To purify PadA from *S. gordonii*, plasmid pMSP-*padA* was used as template in inverse PCR with 5' phosphorylated primers His.*padAR* 5'ATGATGATGTGCTCCGTCTTTAATAGATG and His.*padAF* CACCACCACTAACTCGAGGAATTAGGTTG to substitute the sequence encoding the PadA wall anchorage motif (LPKTG) with a sequence encoding $\times 6$ His (underlined in primers), followed by a stop codon. Amplicons were ligated following removal of original template by DpnI digestion, and resulting plasmids were transformed into *E. coli* JM109. Several plasmids were confirmed by sequencing, and then transformed into *S. gordonii* UB2723 $\Delta padA$. A representative strain was selected in which *padA* gene expression was induced with nisin (50 ng ml^{-1}), and PadA protein, in the absence of cell wall anchorage motif, was secreted into the growth medium (Figure S1).

Generation of plasmid pMSP-*hsa* carrying the complete coding sequence of *hsa* and *S. gordonii* strain Δhsa /pMSP-*hsa* (UB1746) have been described previously (Jakubovics et al., 2009). To make a

complement in *S. gordonii* UB2773 $\Delta hsa \Delta padA$ double mutant, pMSP-*hsa* was transformed into this strain to generate *S. gordonii* UB2777 $\Delta hsa \Delta padA$ /pMSP-*hsa*. The *S. gordonii* pMSP-*hsa* complemented strains were induced with nisin ($10\text{--}50 \text{ ng ml}^{-1}$) and subjected to lectin immunoblotting with sWGA to confirm Hsa expression (Jakubovics et al., 2009; Figure 2).

4.4 | Site-directed mutagenesis and protein expression

Site-directed mutagenesis of two potential integrin-recognition sites in the F2 N-terminal region of PadA have been previously described (Keane et al., 2013). Briefly, alanine-substitution mutagenesis was performed by the use of mutagenic primers containing base mismatches in inverse PCR amplification of pET46-F2, containing the PadA-F2 domain coding sequence to generate pET46-F2 NGR_{AAA}, pET46-F2 RGT_{AAA} or pET46-F2 AGD_{AAA}. In addition to the base mismatches corresponding to the alanine substitutions, a new engineered restriction site was introduced into each plasmid, enabling restriction digest to generate compatible ends for self-ligation to reform a circular plasmid.

A modified alanine substitution method was employed to generate double and triple motif substitutions. In summary, this technique avoided the need for restriction digests to prepare complementary ends and instead made use of 5' phosphate groups on the primers to enable plasmid self-ligation. pET46-F2 AGD_{AAA} was extracted and purified from *E. coli* JM109 and used as template DNA for inverse PCR amplification using primers JH5F/JH6R. These primers incorporated 5' phosphate groups and base mismatches to generate both the alanine substitutions and an engineered AgeI site to facilitate screening by restriction digest analysis. Phusion DNA Polymerase (Life Technologies, Paisley, UK) was used in a two-step protocol to generate the desired amplicon of 7200 bp. This was treated with DpnI for 1 hr at 37°C to remove template DNA and subsequently purified. The purified DNA was self-ligated using T4 DNA ligase for 16 hr at 16°C and subsequently transformed into competent *E. coli* JM109 cells. Transformants were selected for Ap^R , and colonies were screened for plasmids that were cut with AgeI, indicating the formation of pET46-F2 RGT_{AAA}AGD_{AAA}, and this was confirmed by sequencing. Purified plasmid was then transformed into competent *E. coli* BL21 cells for recombinant protein production (see below).

Generation of a pET46-F2 NGR_{AAA}RGT_{AAA}AGD_{AAA} plasmid construct was achieved using a similar alanine substitution technique to that used to generate the pET46-F2 RGT_{AAA}AGD_{AAA} construct. Briefly, the template plasmid pET46-F2 RGT_{AAA}AGD_{AAA} was extracted and purified from *E. coli* JM109. 5'-phosphate-modified JH19F and JH20R primers, which incorporated an engineered NotI restriction site, were used in Phusion PCR to generate the desired amplicon (7200 bp), which was subsequently treated with DpnI, self-ligated and transformed into competent *E. coli* JM109 cells. Plasmids from transformant cells were extracted, purified, and analysed by NotI restriction digest. Plasmids that gave the correct NotI restriction digest pattern were likely to be the desired constructs. This was confirmed by sequencing, before transformation of individual plasmids into competent *E. coli* BL21 cells.

4.5 | Protein expression and purification

Recombinant protein expression was induced in *E. coli* BL21 cultures at OD₆₀₀ 0.5–0.7 by adding IPTG at a final concentration of 1 mM, and continuing incubation for 4 hr at 37°C with shaking at 220 rpm. Cells were harvested by centrifugation (5000 × g, 10 min), and the pellet was lysed in 2 ml Buffer B (8 M urea, 0.1 M NaH₂PO₄, 0.01 M Tris-HCl, pH 7.0) supplemented with 0.1 M phenylmethanesulfonylfluoride (PMSF) at room temperature for 4 hr. Cell debris was removed by centrifugation (12,000 × g, 15 min). Ni-NTA agarose (Qiagen; 300 µl) was added to 2 ml lysis supernatant, mixed gently at room temperature for 25 min, and then transferred to a polypropylene column (Qiagen). The column was washed with 4 ml Buffer B (supplemented with 20 mM imidazole) and then twice with Buffer C (1 M NaCl, 10% EtOH, 2% Tween-20) supplemented with 20 mM imidazole. Protein was eluted six times with Buffer D (Buffer B, supplemented with 100 mM imidazole). All of the washes and eluted fractions were collected and analysed by SDS-PAGE. Fractions containing recombinant proteins were pooled and dialysed against dH₂O supplemented with protease inhibitor cocktail (Sigma). Dialysed protein solutions were freeze-dried, suspended in dH₂O, and the protein concentrations determined using the Bradford assay (BioRad Laboratories, Hemel Hempstead, Herts, UK).

4.6 | PadA_{6His} expression and purification from *S. gordonii*

S. gordonii UB2870 Δ padA/pMSP-padA_{6His} cultures were grown in TY-Glc medium at 37°C with Sp, Em and 100 ng ml⁻¹ nisin, to early stationary phase. The cultures were centrifuged (12,000 × g, 4°C, 20 min), the supernatants were collected, protease inhibitor cocktail (Sigma) added, and then passed through a 0.45 µm filter. The fluid was concentrated to 4 ml, using a centrifugal filter unit, and centrifuged (12,000 × g, 4°C, 10 min) to remove particulate matter. The fluid was then dialysed into Buffer A (50 mM Tris, 200 mM NaCl, 10% glycerol, 0.1% Triton X-100, pH 7.5) for 16 hr at 4°C. A HiTrap Ni²⁺ affinity column (GE Healthcare, Cardiff, UK) was pre-equilibrated in Buffer A, the protein sample was loaded onto the column, and non-specifically bound proteins were removed by washing the column first with Buffer A (5 ml) and then with Buffer B (50 mM Tris, 200 mM NaCl, 10% glycerol, 0.1% Triton X-100, 20 mM imidazole, pH 7.5). The PadA_{6His} protein was eluted with 15 ml Buffer C (50 mM Tris, 200 mM NaCl, 10% glycerol, 0.1% Triton X-100, 500 mM imidazole, pH 7.5) and collected in 3 ml fractions. These were analysed by SDS-PAGE and fractions containing pure PadA_{6His} were pooled and dialysed into Buffer A for 16 hr at 4°C. Identity and purity were confirmed by liquid chromatography-mass spectrometry (LC-MS) analysis (University of Bristol Proteomics Facility).

4.7 | Pull-down assay

Dynabeads® His-Tag Isolation and Pulldown kit (Life Technologies) was used for PadA-serum pull-down assays according to the manufacturer's recommended instructions. PadA_{6His} (4 mg ml⁻¹) was diluted in Binding/Wash buffer and incubated with mixed pooled human plasma (TCS Biosciences, Botolph Claydon, Bucks, UK) diluted 1:5 in Pull-down buffer. Elution steps were performed according to the manufacturer's instructions.

4.8 | Mass spectrometry sample preparation

To prepare the eluted samples from the pull-down assays for MS, the samples were subjected to SDS-PAGE until the dye-front had moved 1.5 cm into the gel. The gel was stained with Coomassie blue, destained, and a single gel slice encompassing proteins below 350 kDa was excised. The slice was subjected to in-gel tryptic digestion with a ProGest automated digestion unit (Digilab UK). The resulting peptides were fractionated with a Dionex Ultimate 3000 nanoHPLC system in line with an LTQ-Orbitrap Velos mass spectrometer (Thermo Scientific) controlled by Xcalibur 2.1 software (Thermo Scientific). The Orbitrap was set to analyse the survey scans at 60,000 resolution (at m/z 400) in the mass range m/z 300 to 2,000 and the top twenty multiply-charged ions in each duty cycle were selected for MS/MS in the LTQ linear ion trap.

4.9 | Liquid chromatography-mass spectrometry data analysis

The raw data files were processed and quantified using Proteome Discoverer software v1.2 (Thermo Scientific) and searched against the UniProt/SwissProt *S. gordonii* (strain Challis/ATCC 35105/CH1/DL1/V288) database (2,056 entries) and the UniProt/SwissProt *Homo sapiens* database (70,625 entries) using SEQUEST (Ver. 28 Rev. 13) algorithm for the pull-down elution samples. Peptide precursor mass tolerance was set at 10 ppm, and MS/MS tolerance was set at 0.8 Da. Search criteria included carbamidomethylation of cysteine (+57.0214) as a fixed modification and oxidation of methionine (+15.9949) as a variable modification. Searches were performed with full tryptic digestion, and a maximum of one missed cleavage was allowed. The reverse database search option was enabled, and all peptide data were filtered to satisfy false discovery rate (FDR) of 5%. The Proteome Discoverer software generates a reverse "decoy" database from the same protein database, and any peptides passing the initial filtering parameters that were derived from this decoy database are defined as false positive identifications. The minimum cross-correlation factor (Xcorr) filter was readjusted for each individual charge state separately to optimally meet the predetermined target FDR of 5% based on the number of random false positive matches from the reverse decoy database. Thus, each data set has its own passing parameters.

4.10 | Platelet adherence assay

Whole blood was collected from six donors and added to 1.5 ml acid citrate dextrose per 10 ml blood collected. The donors were healthy subjects who had abstained from taking any non-steroidal anti-inflammatory drugs (NSAIDs) in the previous 10 days. Informed consent was obtained from all subjects, and the study was approved by the Royal College of Surgeons in Ireland Ethics Committee (REC679b). Blood was centrifuged (150 × g, 10 min), and the upper platelet-containing fraction was carefully removed to a fresh tube. The platelet-rich plasma (PRP; collected in acid-citrate dextrose, ACD) was adjusted to pH 6.5 with ACD. Apyrase (1 U ml⁻¹), and prostaglandin-E1 (Sigma Aldrich; 2 µM) were added to the PRP, and the sample was centrifuged (650 × g, 10 min, 20°C). The upper layer containing

platelet-poor plasma was removed, and the platelet pellet was suspended in 2 ml modified HEPES-Tyrod buffer (JNL; 6 mM dextrose, 130 mM NaCl, 9 mM NaHCO₃, 10 mM Na citrate, 10 mM Tris base, 3 mM KCl, 0.8 mM KH₂PO₄, 0.9 mM MgCl₂, pH 7.4). The platelet suspension was then applied to a chromatography column containing 5 ml packed Sepharose 2B-300, previously equilibrated with JNL buffer. The platelet concentration was determined using a Sysmex-100 particle counter (Sysmex, Kobe, Japan).

Static platelet adhesion assay was performed as described previously (Kerrigan et al., 2002). Briefly, 96-well plates were coated with bacteria (1×10^9 cells ml⁻¹), recombinant protein fragments, fibrinogen, or BSA (each at 100 µg ml⁻¹). Gel-filtered platelets (4×10^8 cells ml⁻¹) were added to each well and incubated for 45 min at 37°C. Following a gentle wash to remove unattached platelets, lysis buffer containing *p*-nitrophenol phosphate was added to the wells and incubated for 20 min at 37°C. The resultant absorbance at 405 nm (A_{405}) was a measure of acid phosphatase activity, proportional to numbers of platelets bound. Where appropriate, platelets were activated with 20 µM TRAP sequence SFLLRN (Sigma Aldrich, Wexford, Ireland).

4.11 | Platelet spreading assay

Poly-L-lysine-coated glass slides were coated with PadA protein fragment (100 µg ml⁻¹) for 16 hr at 4°C. Slides were then blocked with 1% BSA; washed and gel-filtered platelets (5×10^6 platelets ml⁻¹) were allowed to spread on the PadA fragments for 45 min at 37°C. The slides were washed, the platelets were fixed and permeabilized, and then the samples were stained with Alexa 546 phalloidin and examined by confocal microscopy as described in detail elsewhere (Keane et al., 2013). The percentage of platelets spread was calculated from five areas, selected randomly, containing 200 or more total cells.

4.12 | Bacterial cell adhesion assays

Extracellular matrix proteins in coating buffer (20 mM Na₂CO₃, 2 mM NaHCO₃, pH 9.3) were added to the wells of a high-binding 96-well plate (Immulon 2HB) and incubated for 16 hr at 4°C. In some experiments, immobilized substrata were then desialylated with 0.001 U neuraminidase from *Clostridium perfringens* (Sigma) in 0.1 M sodium acetate buffer (pH 5.0) containing 2 mM CaCl₂, for 2 hr at 37°C. Wells were washed once in TBSC (10 mM Tris-HCl pH 7.6, 0.15 M NaCl, 5 mM CaCl₂), and non-specific binding sites blocked with 3% BSA in TBSC containing 0.05% Tween-20 (TBST) for 1 hr at 37°C. Bacterial cultures were grown for 16 hr at 37°C, and cells were harvested by centrifugation (5000 × *g*, 7 min). Cells were washed once in TBSC, adjusted to OD₆₀₀ 0.5, and portions (0.1 ml) incubated with the immobilized proteins at 37°C for 2 hr. The suspensions were then removed, and the wells were washed twice in TBS. Adherent cells were fixed with 25% formaldehyde for 30 min at room temperature. Wells were washed twice in TBS, 0.5% crystal violet was added, and the plates were incubated for 2 min at room temperature. Wells were washed three times in TBS, 10% acetic acid (0.1 ml) was added and after 5 min, levels of adhesion were quantified by measuring absorbance at 595 nm (A_{595}). Previous work has shown that bacterial cell

numbers are proportional to A_{595} over the range employed in the assays (Jakubovics et al., 2005).

4.13 | Salivary pellicle adhesion assay

Saliva was collected from at least six healthy adult human subjects, who provided written informed consent (approved by the National Research Ethics Committee South Central Oxford C. 165 # 08/H0606/87 + 5). Exclusion criteria were: antimicrobial medication within 7 days previously, continuous medication, gross dental caries, or unstable periodontal disease. Samples were pooled, mixed with 0.25 M dithiothreitol on ice for 10 min and clarified by centrifugation (8000 × *g*, 10 min). The supernatant was diluted to 10% with sterile water, filter sterilized (0.22 µm pore membrane) and aliquots were stored at -20°C.

Saliva-coated cover slips were prepared by placing sterile 19-mm-diameter cover slips (Menzel-Glaser, Braunschweig, Germany) into 12-well plates (Greiner) and adding 10% saliva (1 ml) to each well. The cover slips were incubated at 4°C for 16 hr, washed with PBS, and transferred to a fresh 12-well plate. Bacterial cell suspension (OD₆₀₀ 0.5) was added to each well as described above, incubated at 37°C for 2 hr, and aspirated from the wells, and the cover slips were washed twice in TBSC. Adherent cells were fixed and stained with crystal violet, and levels of adhesion were quantified by A_{595} measurement.

4.14 | Biofilm formation

Bacterial cultures grown for 16 hr (10 ml) were harvested by centrifugation (5000 × *g*, 7 min), washed in modified C (mC) medium (0.25% Difco Proteose Peptone #2, 0.75% yeast extract, 10 mM K₂HPO₄, 0.4 mM MgSO₄·7H₂O, 17 mM NaCl, pH 7.5, containing 0.2% glucose) and adjusted to OD₆₀₀ 1.0 in mC medium. Saliva-coated cover slips were prepared as above in 12-well plates (Greiner) before bacterial cell suspension (OD₆₀₀ 0.5) was added to each well. The plates were incubated at 37°C for 1 hr with shaking at 50 r.p.m. The cell suspensions were removed and the cover slips washed twice in mC medium. Fresh mC medium was then added to each well and the plates were incubated at 37°C for a further 15 hr. Cover slips were then removed, washed twice in PBS, and stained with crystal violet as described above.

4.15 | Recombinant protein binding assays

ECM proteins in coating buffer (50 µl) were added to wells of a high-binding 96-well plate (Immulon 2HB) and incubated for 16 hr at 4°C. Wells were washed once in TBSC and non-specific binding sites were blocked with 3% BSA in TBSC for 1 hr at 37°C. Wells were washed once in TBSC and recombinant protein (0–5 µg) diluted in TBSC was applied to the wells and incubated for 1 hr at 37°C. Unbound protein was removed and wells washed once in TBS. Primary antibody diluted in TBST was added to the wells and incubated for 1 hr at 37°C. Wells were washed twice in TBST before adding HRP-linked secondary antibody diluted in TBST containing 3% BSA and incubating for 1 hr at 37°C. Wells were washed once in TBST, twice in TBS, and detection reagent (0.102 M Na₂HPO₄, 0.049 M citric acid, 0.012% H₂O₂, 3.7 mM o-

phenylenediamine) was added to wells. Plates were incubated in the dark for 10 min at room temperature, 0.56 M H₂SO₄ was added to stop the reactions and A₄₉₀ measured. x6His-tagged proteins were detected using anti-tetraHis antibody (Qiagen) at 1:1000 dilution and HRP-conjugated anti-mouse antibody (Dako) at 1:2000 dilution. Fibrinogen was detected using rabbit anti-human fibrinogen antibody (Dako) at 1:1000 dilution and HRP-conjugated swine anti-rabbit antibody (Dako) at 1:2000 dilution.

ACKNOWLEDGMENTS

We thank Lindsay Dutton for excellent technical assistance, Mutanu Malinda for performing pull-down experiments, Gary Dunny for the provision of plasmid pMSP7517, and Thea Tilley and Cormac McDonnell for invaluable help and advice. We gratefully acknowledge receipt of funding from The Wellcome Trust of a Clinical Training Fellowship #097285 for J.A.H.

CONFLICT OF INTEREST

The authors declare no conflicts of interest.

REFERENCES

- Arman, M., Krauel, K., Tilley, D. O., Weber, C., Cox, D., Greinacher, A., ... Watson, S. P. (2014). Amplification of bacteria-induced platelet activation is triggered by FcγRIIA, integrin αIIbβ₃, and platelet factor 4. *Blood*, 123, 3166–3174.
- Bensing, B. A., & Sullam, P. A. (2002). An accessory *sec* locus of *Streptococcus gordonii* is required for export of the surface protein GspB and for normal levels of binding to human platelets. *Molecular Microbiology*, 44, 1081–1094.
- Bensing, B. A., López, J. A., & Sullam, P. A. (2004). The *Streptococcus gordonii* surface proteins GspB and Hsa mediate binding to sialylated carbohydrate epitopes on the platelet membrane glycoprotein Iba. *Infection and Immunity*, 72, 6528–6537.
- Brown, S. L., Lundgren, C. H., Nordt, T., & Fujii, S. (1994). Stimulation of migration of human aortic smooth muscle cells by vitronectin: Implications for atherosclerosis. *Cardiovascular Research*, 28, 1815–1820.
- Bryan, E. M., Bae, T., Kleerebezem, M., & Dunny, G. M. (2000). Improved vectors for nisin-controlled expression in gram-positive bacteria. *Plasmid*, 44, 183–190.
- Cahill, T. J., & Prendergast, B. D. (2015). Infective endocarditis. *Lancet*, 387, 882–893.
- Cognasse, H. H., Damien, P., Chabert, A., Pozzetto, B., Cognasse, F., & Garraud, O. (2015). Platelets and infections – complex interactions with bacteria. *Frontiers in Immunology*, 6, 82.
- Cox, D., Kerrigan, S. W., & Watson, S. P. (2011). Platelets and the innate immune system: Mechanisms of bacterial-induced platelet activation. *Journal of Thrombosis and Haemostasis*, 9, 1097–1107.
- Deng, L., Bensing, B. A., Thamadilok, S., Yu, H., Lau, K., Chen, X., ... Varki, A. (2014). Oral streptococci utilize a Siglec-like domain of serine-rich repeat adhesins to preferentially target platelet sialoglycans in human blood. *PLoS Pathogens*, 19, e1004540.
- Ekmeççi, Ö. B., & Ekmeççi, H. (2006). Vitronectin in atherosclerotic disease. *Clinica Chimica Acta*, 368, 77–83.
- Fitzgerald, J. R., Foster, T. J., & Cox, D. (2006). The interaction of bacterial pathogens with platelets. *Nature Reviews Microbiology*, 4, 445–457.
- Haisman, R. J., & Jenkinson, H. F. (1991). Mutants of *Streptococcus gordonii* Challis over-producing glucosyltransferase. *Journal of General Microbiology*, 137, 483–489.
- Hanahan, D. (1983). Studies on transformation of *Escherichia coli* with plasmids. *Journal of Molecular Biology*, 166, 557–580.
- Henderson, B., Nair, S., Pallas, J., & Williams, M. A. (2011). Fibronectin: A multidomain host adhesin targeted by bacterial fibronectin-binding proteins. *FEMS Microbiology Reviews*, 35, 147–200.
- Hirt, H., Erlandsen, S. L., & Dunny, G. M. (2000). Heterologous inducible expression of *Enterococcus faecalis* pCF10 aggregation substance Asc10 in *Lactococcus lactis* and *Streptococcus gordonii* contributes to cell hydrophobicity and adhesion to fibrin. *Journal of Bacteriology*, 183, 2299–2306.
- Jakubovics, N. S., Kerrigan, S. W., Nobbs, A. H., Strömberg, N., van Dolleweerd, C. J., Cox, D. M., ... Jenkinson, H. F. (2005). Functions of cell surface-anchored antigen I/II family and Hsa polypeptides in interactions of *Streptococcus gordonii* with host receptors. *Infection and Immunity*, 73, 6629–6638.
- Jakubovics, N. S., Brittan, J. L., Dutton, L. C., & Jenkinson, H. F. (2009). Multiple adhesin proteins on the cell surface of *Streptococcus gordonii* are involved in adhesion to human fibronectin. *Microbiology*, 155, 3572–3580.
- Jenkinson, H. F. (1987). Novobiocin-resistant mutants of *Streptococcus sanguis* with reduced cell hydrophobicity and defective in coaggregation. *Journal of General Microbiology*, 133, 1909–1918.
- Jenkinson, H. F. (2011). Beyond the oral microbiome. *Environmental Microbiology*, 13, 3077–3087.
- Jenne, C. N., & Kubes, P. (2015). Platelets in inflammation and infection. *Platelets*, 26, 286–292.
- Jung, C.-J., Yeh, C.-Y., Hsu, R.-B., Lee, C.-M., Shun, C.-Y., & Cia, J.-S. (2015). Endocarditis pathogen promotes vegetation formation by inducing intravascular neutrophil extracellular traps through activated platelets. *Circulation*, 131, 571–581.
- Keane, C., Petersen, H., Reynolds, K., Newman, D. K., Cox, D., Jenkinson, H. F., ... Kerrigan, S. W. (2010). Mechanism of outside-in αIIbβ₃-mediated activation of human platelets by the colonizing bacterium, *Streptococcus gordonii*. *Arteriosclerosis, Thrombosis, and Vascular Biology*, 30, 2408–2415.
- Keane, C., Petersen, H. J., Tilley, D. O., Haworth, J., Cox, D., Jenkinson, H. F., & Kerrigan, S. W. (2013). Multiple sites on *Streptococcus gordonii* surface protein PadA bind to platelet GPIIb/IIIa. *Thrombosis and Haemostasis*, 110, 1278–1287.
- Kerrigan, S. W. (2015). The expanding field of platelet-bacterial interactions. *Platelets*, 26, 293–301.
- Kerrigan, S. W., & Cox, D. (2010). Platelet-bacterial interactions. *Cellular and Molecular Life Sciences*, 67, 513–523.
- Kerrigan, S. W., Douglas, I., Wray, A., Heath, J., Byrne, M. F., Fitzgerald, D., & Cox, D. (2002). A role for glycoprotein IIb in *Streptococcus sanguis*-induced platelet aggregation. *Blood*, 100, 509–516.
- Kerrigan, S. W., Jakubovics, N. S., Keane, C., Maguire, P., Wynne, K., Jenkinson, H. F., & Cox, D. (2007). Role of *Streptococcus gordonii* surface proteins SspA/SspB and Hsa in platelet function. *Infection and Immunity*, 75, 5740–5747.
- Lockhart, P. B., Brennan, M. T., Thornhill, M., Michalowicz, B. S., Noll, J., Bahrani-Mougeot, F. K., & Sasser, H. C. (2009). Poor oral hygiene as a risk factor for infective endocarditis-related bacteremia. *Journal of the American Dental Association*, 140, 1238–1244.
- Mazmanian, S. K., Ton-That, H., & Schneewind, O. (2001). Sortase-catalysed anchoring of surface proteins to the cell wall of *Staphylococcus aureus*. *Molecular Microbiology*, 40, 1049–1057.
- McNab, R., Forbes, H., Handley, P. S., Loach, D. M., Tannock, G. W., & Jenkinson, H. F. (1999). Cell wall-anchored CshA polypeptide (259 kilodaltons) in *Streptococcus gordonii* forms surface fibrils that confer hydrophobic and adhesive properties. *Journal of Bacteriology*, 181, 3087–3095.
- McNicol, A. (2015). Bacteria-induced intracellular signalling in platelets. *Platelets*, 26, 309–316.
- McNicol, A., & Israels, S. J. (2010). Mechanisms of oral bacteria-induced platelet activation. *Canadian Journal of Physiology and Pharmacology*, 88, 510–524.

- Moreillon, P., & Que, Y. A. (2004). Infective endocarditis. *Lancet*, 363, 139–149.
- Moriarty, R., McManus, C. A., Lambert, M., Tilley, T., Devocelle, M., Brennan, M., ... Cox, D. (2015). A novel role for the fibrinogen Asn-Gly-Arg (NGR) motif in platelet function. *Thrombosis and Haemostasis*, 113, 290–304.
- Muñoz, P., Kestler, M., de Alarcon, A., Miro, J. M., Bermejo, J., Rodríguez-Abella, H., ... Bouza, E. (2015). Current epidemiology and outcome of infective endocarditis: A multicentre, prospective, cohort study. *Medicine (Baltimore)*, 94, e1816.
- Nilson, B., Olaison, L., & Rasmussen, M. (2015). Clinical presentation of infective endocarditis caused by different groups on non-beta haemolytic streptococci. *European Journal of Clinical Microbiology & Infectious Diseases*, 35, 215–218.
- Nobbs, A. H., Lamont, R. J., & Jenkinson, H. F. (2009). *Streptococcus* adherence and colonization. *Microbiology and Molecular Biology Reviews*, 73, 407–450.
- Ogawa, H., Yoneda, A., Seno, N., Hayashi, M., Ishizuka, I., Hase, S., & Matsumoto, I. (1995). Structures of the N-linked oligosaccharides on human plasma vitronectin. *European Journal of Biochemistry*, 230, 994–1000.
- Pampolina, C., & McNicol, A. (2005). *Streptococcus sanguis*-induced platelet activation involves two waves of tyrosine phosphorylation mediated by FcγRIIA and α_{IIb}β₃. *Thrombosis and Haemostasis*, 93, 932–939.
- Parker, C. J., Stone, O. L., White, V. F., & Seinshaw, N. J. (1989). Vitronectin (S protein) is associated with platelets. *British Journal of Haematology*, 71, 245–252.
- Petersen, H. J., Keane, C., Jenkinson, H. F., Vickerman, M. M., Jesionowski, A., Waterhouse, J. C., ... Kerrigan, S. W. (2010). Human platelets recognize a novel surface protein, PadA, on *Streptococcus gordonii* through a unique interaction involving fibrinogen receptor GPIIb/IIIa. *Infection and Immunity*, 78, 413–422.
- Plummer, C., Wu, H., Kerrigan, S. W., Meade, G., Cox, D., & Douglas, C. W. I. (2005). A serine-rich glycoprotein of *Streptococcus sanguis* mediates adhesion to platelets via GPIb. *British Journal of Haematology*, 129, 101–109.
- Podbielski, A., Spellerberg, B., Woischnik, M., Pohl, B., & Lütticken, R. (1996). Novel series of plasmid vectors for gene inactivation and expression analysis in group A streptococci (GAS). *Gene*, 177, 137–147.
- Pyburn, T. M., Bensing, B. A., Xiong, Y. Q., Melancon, B. J., Tomasiak, T. M., Ward, N. J., ... Iverson, T. M. (2011). A structural model for binding of the serine-rich repeat adhesin GspB to host carbohydrate receptors. *PLoS Pathogens*, 7, e1002112.
- Reheman, A., Gross, P., Yang, H., Chen, P., Allen, D., Leytin, V., ... Ni, H. (2005). Vitronectin stabilizes thrombi and vessel occlusion but plays a dual role in platelet aggregation. *Journal of Thrombosis and Haemostasis*, 3, 875–883.
- Seo, H. S., Minasov, G., Seepersaud, R., Doran, K. S., Dubrovskaya, I., Shuvalova, L., ... Sullam, P. M. (2013). Characterization of fibrinogen binding by glycoproteins Srr1 and Srr2 of *Streptococcus agalactiae*. *The Journal of Biological Chemistry*, 288, 35982–35996.
- Singh, B., Su, Y.-C., & Riesbeck, K. (2010). Vitronectin in bacterial pathogenesis: A host protein used in complement escape and cellular invasion. *Molecular Microbiology*, 78, 545–560.
- Slipczuk, L., Codolosa, J. N., Davila, C. D., Romero-Corral, A., Yun, J., Pressman, G. S., & Figueredo, V. M. (2013). Infective endocarditis epidemiology over five decades: a systematic review. *PLoS One*, 8, e82665.
- Takahashi, Y., Konishi, K., Cisar, J. O., & Yoshikawa, M. (2002). Identification and characterization of hsa, the gene encoding the sialic acid-binding adhesin of *Streptococcus gordonii* DL1. *Infection and Immunity*, 70, 1209–1218.
- Takahashi, Y., Yajima, A., Cisar, J. O., & Konishi, K. (2004). Functional analysis of the *Streptococcus gordonii* DL1 sialic acid-binding adhesin and its essential role in bacterial binding to platelets. *Infection and Immunity*, 72, 3876–3882.
- Takamatsu, D., Bensing, B. A., Cheng, H., Jarvis, G. A., Siboo, I. R., Lopez, J. A., ... Sullam, P. M. (2005). Binding of the *Streptococcus gordonii* surface glycoproteins GspB and Hsa to specific carbohydrate structures on platelet membrane glycoprotein Iba. *Molecular Microbiology*, 58, 380–392.
- Takamatsu, D., Bensing, B. A., Prakobphol, A., Fisher, S. J., & Sullam, P. A. (2006). Binding of the streptococcal surface glycoproteins GspB and Hsa to human salivary proteins. *Infection and Immunity*, 74, 1933–1940.
- Thiagarajan, P., & Kelly, K. L. (1988). Exposure of binding sites for vitronectin on platelets following stimulation. *The Journal of Biological Chemistry*, 263, 3035–3038.
- Tilley, D. O., Arman, M., Smolenski, A., Cox, D., O'Donnell, J. S., Douglas, C. W., ... Kerrigan, S. W. (2013). Glycoprotein Iba and FcγRIIa play key roles in platelet activation by the colonizing bacterium, *Streptococcus oralis*. *Journal of Thrombosis and Haemostasis*, 11, 941–950.
- To, W. S., & Midwood, K. S. (2011). Plasma and cellular fibronectin: Distinct and independent functions during tissue repair. *Fibrogenesis & Tissue Repair*, 4, 21.
- Wright, C. J., Burns, L. H., Jack, A. A., Back, C. R., Nobbs, A. H., Lamont, R. J., & Jenkinson, H. F. (2013). Microbial interactions in building of communities. *Molecular Oral Microbiology*, 28, 83–101.
- Xiong, Y. Q., Bensing, B. A., Bayer, A. S., Chambers, H. F., & Sullam, P. A. (2008). Role of the serine-rich surface glycoprotein GspB of *Streptococcus gordonii* in the pathogenesis of infective endocarditis. *Microbial Pathogenesis*, 45, 297–301.
- Zhou, M., & Wu, H. (2009). Glycosylation and biogenesis of a family of serine-rich bacterial adhesins. *Microbiology*, 155, 317–327.
- Zhou, P., Liu, J., Li, X., Takahashi, Y., & Qi, F. (2015). The sialic acid binding protein, Hsa, in *Streptococcus gordonii* DL1 also mediates intergeneric coaggregation with *Veillonella* species. *PLoS One*, 10, e0143898.

SUPPORTING INFORMATION

Additional Supporting Information may be found online in the supporting information tab for this article.

How to cite this article: Haworth, J. A., Jenkinson, H. F., Petersen, H. J., Back, C. R., Brittan, J. L., Kerrigan, S. W., and Nobbs, A. H. (2017), Concerted functions of *Streptococcus gordonii* surface proteins PadA and Hsa mediate activation of human platelets and interactions with extracellular matrix, *Cellular Microbiology*, 19, e12667. doi: 10.1111/cmi.12667